

## EVOLUTION OF INTERMEDIATE MASS CLOSE BINARIES

Th.J. van der Linden  
Astronomical Institute, University of Amsterdam

### Abstract

Numerical simulations of close binary evolution were performed for five binary systems, using a newly developed evolutionary program. The systems have masses 3+2, 4+3.2, 6+4, 9+6, 12+8  $M_{\odot}$  and periods 2<sup>d</sup>, 1<sup>d</sup>78, 3<sup>d</sup>, 4<sup>d</sup>, 5<sup>d</sup> respectively. The primary component was followed from the zero-age main sequence through the mass transfer phase to core-helium burning. Special care was given to the self-consistent determination of the mass transfer rate and the detailed treatment of composition changes. After the mass transfer phase the resulting systems consist of a main sequence star with a helium star companion of mass 0.36, 0.46, 0.82, 1.48, 2.30  $M_{\odot}$  for the five systems respectively. Interesting "thermal pulses" were found in the 3+2  $M_{\odot}$  system at the onset of helium burning.

### Introduction

Most theoretical studies of the evolution of close binaries have so far been restricted to systems with high ( $M > 15 M_{\odot}$ ) and low-mass ( $M < 3 M_{\odot}$ ) primaries. The high-mass systems evolve into Wolf-Rayet binaries, while the low-mass systems lead to Algol-type systems and further to systems containing a white dwarf (cf. Paczynski 1971; Thomas 1978). The intermediate mass (3-15  $M_{\odot}$  primaries) close binaries are of particular importance, as they cover the entire B spectral range, and so far were studied in only a very few cases (Kippenhahn and Weigert 1967; Harmanec 1970; Plavec, Ulrich and Polidan 1973). As still little is known about the final evolutionary stages of these systems, a new evolutionary program was constructed which enables us to use as much (nuclear) input physics as is necessary to carry out reliable computations for the advanced evolutionary stages. Our calculation include all the effects of mass transfer, nuclear burning and composition changes in a completely self-consistent way. Evolutionary sequences were calculated for five systems, which cover the mass range of 3-12  $M_{\odot}$  for the primary, assuming conservative mass transfer and choosing periods such that mass transfer starts as Case B and at a time when the outer layers are still in radiative

equilibrium. Mass ratios were chosen such that no problems were expected with the accreting companion star (cf. Kippenhahn & Meyer-Hoffmeister 1977). The initial composition used was  $X = 0.70$  and  $Z = 0.03$ .

### Input physics and numerical techniques

For the equation of state the contributions due to electrons ions and photons are taken into account. The thermodynamic properties of the electrons gas are used in tabular form, allowing for partial as well as relativistic degeneracy. The contributions from the ions and photons are calculated analytically. The cross-sections used for the nuclear reactions were taken from the expressions given by Fowler et al. (1975). Absorption coefficients were interpolated from the tables of Cox and Stewart (1969), using 2 point interpolation. The program used obtains a fully implicit solution of the structure equations. Composition changes are calculated algebraically by solving a diffusion equation (which includes a complete thermonuclear reaction network) simultaneously with all other structure equations. Implicit boundary points are used for all convective zones (central as well as surface and intermediate convection zones). An abbreviated nuclear network was used for PP and CNO-cycles, except for the  $12+8 M_{\odot}$  system where all of the 14 reactions in the CNO-bicycle were treated separately. All equations were solved algebraically with a Newton-Raphson scheme using a tridiagonal (Jacobi) matrix system devised by R.J. Takens. The central boundary conditions used are described by Savonije and Takens (1976). Surface boundary conditions used are similar to those described by Savonije (1978). A more detailed description of input physics and numerical techniques will be given elsewhere.

### Discussion

The mass loss rates as determined by using implicit boundary condition are shown in figure 2. All curves show a double peaked structure. The second peak in these curves is caused by the onset of convection in the outer layers. In the  $3 M_{\odot}$  primary and the  $4 M_{\odot}$  primary deep surface convection occurs when the stars have almost reached their minimum luminosity in the HR-diagram, giving rise to an increased mass transfer rate during the second part of the mass transfer. In the  $6,9,12 M_{\odot}$  system no deep surface convection occurs during mass transfer. The increase of the mass transfer rate here is due to the increase in size of the small convection zone present in the atmosphere, the extend of which is controlled by the luminosity of the star. In the time following minimum luminosity the extending atmospheric convection gives rise to an extension of the rapid mass transfer phase.

The tracks of the mass losing star in the HR-diagram show some systematic trends. They all show the familiar drastic decrease in luminosity during the rapid mass transfer phase due to the absorption of radiation energy in the outflowing atmosphere. Mass transfer terminates at the onset of core helium burning after which the star relaxes to its

thermal equilibrium position near the helium main sequence. The low mass remnants are very faint in comparison to their newly formed companion. This is clearly demonstrated in Table 1, which shows that for the lower-mass systems the resulting helium star companion will be practically unobservable. A particularly interesting phenomenon occurs at the onset of helium burning in the (original) 3+2  $M_{\odot}$  system. As the mass-losing star in this system becomes degenerate before helium burning, this remnant reacts differently to the onset of helium burning than the other four systems. The mass fraction of the star which becomes convective is shown as a function of time in figure 4. The convective core shows three thermal oscillations before it reaches its final thermal equilibrium state, each oscillation removes a part of the degeneracy. During the oscillations over 50% of the star becomes convective which is about 3 times the extent of the core in thermal equilibrium. The remnant has a hydrogen content  $X \sim 0.50$  in its outer layers after mass transfer, in contrast to the other systems which have  $X \sim 0.20$ . This difference in hydrogen content is responsible for the increase in luminosity by more than one magnitude before settling on the helium main sequence.

Examination of Table 1 shows that in each case the resulting system consists of a newly formed bright main sequence B-star accompanied by a faint helium star in a rather wide ( $P > 60^d$ ) orbit. The difference in luminosity between the two stars is about 5 magnitudes for the low mass-systems and 2 magnitudes for the heavier ones. Due to the faintness of the companion the systems are expected to be unrecognized as a binary in the visible part of the spectrum. Most of the flux of the helium star is emitted in the UV part of the spectrum due to its high surface temperature ( $\log T_{\text{eff}} \sim 4.7$ ). Because of this high UV flux it has been suggested that these systems might appear as Be stars (see Kriz and Harmanec 1975 and references therein). It should be pointed out that this kind of evolution has significant influence on the statistics of B-stars, as every B-star in a binary system produces another B-star of somewhat earlier spectral type, thereby increasing the lifetime of the system as a binary with the primary on the main sequence by about a factor of two. We are presently continuing the evolution of the helium stars in these five systems in order to study the type and composition of their final remnants.

TABLE 1

$M_1, M_2$	$P_i$	$P_f$	$A_f$	$M_{1f}$	$M_2$	$\Delta m$
3+2	2 <sup>d</sup>	93	147	.36	4.64	5.0
4+3.2	1.78	11.8	195	.46	6.74	4.0
6+4	3	96	191	.82	9.18	3.5
9+6	4	78	190	1.48	13.52	2.7
12+8	5	65	184	2.30	17.70	-

### Acknowledgements

It is a pleasure to acknowledge the inspiration and guidance of E.P.J. van den Heuvel throughout this work. I am indebted to R.J. Takens for the introduction to and the use of his algebraic scheme and numerical routines. This work was supported by the Netherlands Organization of Pure Research (Z.W.O.) under projectnumber 78-110.

### References

- Cox, A.N. and Stewart, J.N. 1969, *Sci. Infor. Astr. Council USSR Acad. Sci.* Vol. 15.
- Fowler, W.A., Caughlan, G.R. and Zimmerman, B.A. 1975, *Ann. Rev. Astr. Astrophys.* 13, 69.
- Harmanec, P. 1970, *Bull. Astron. Inst. Czech.* 21, 113.
- Kippenhahn, R. and Weigert, A. 1967, *Z. Astrophys.* 65, 251.
- Kippenhahn, R. and Meyer-Hoffmeister, E. 1977, *Astron. Astrophys.* 54, 539.
- Kriz, S. and Harmanec, P. 1975, *Bull. Astron. Inst. Czech.* 26, 65.
- Paczynski, B.E. 1971, *Ann. Rev. Astron. Astrophys.* 9, 183.
- Plavec, M., Ulrich, R.K. and Polidan, R.S. 1973, *Publ. Astron. Soc. Pac.* 85, 769.
- Savonije, G.J. 1978, *Astron. Astrophys.* 62, 317.
- Savonije, G.J. and Takens, R.J. 1976, *Astron. Astrophys.* 47, 231.
- Thomas, H. 1977, *Ann. Rev. Astron. Astrophys.* 15, 127.

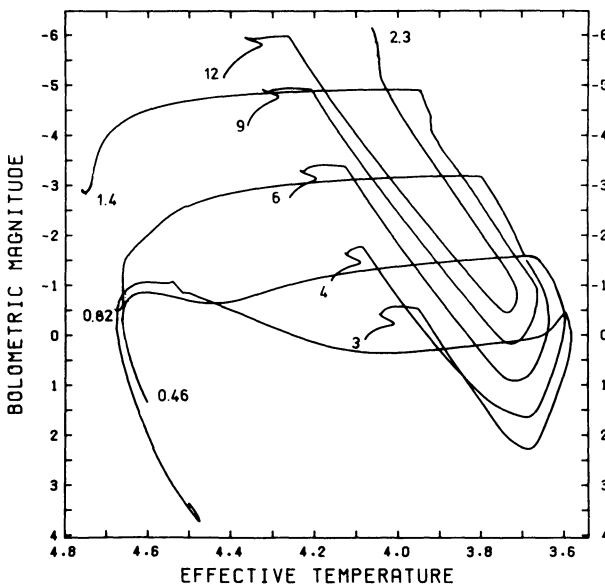


*Fig. 1. Evolutionary tracks of the primary component, from the ZAMS through mass exchange phase to He-main sequence, except for the 12  $M_{\odot}$  track which is terminated at He-ignition.*

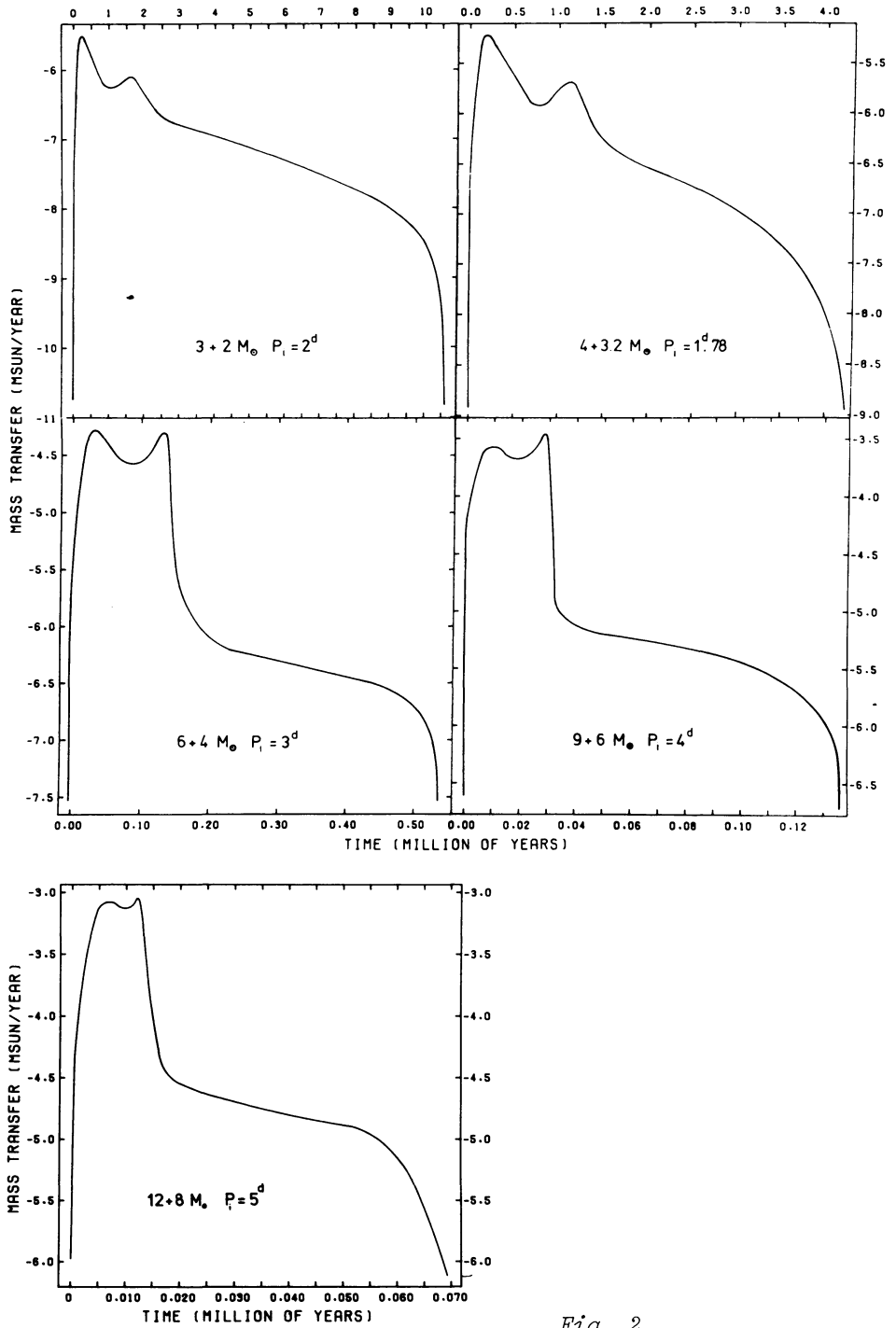


Fig. 2.  
Mass loss rate vs. time.

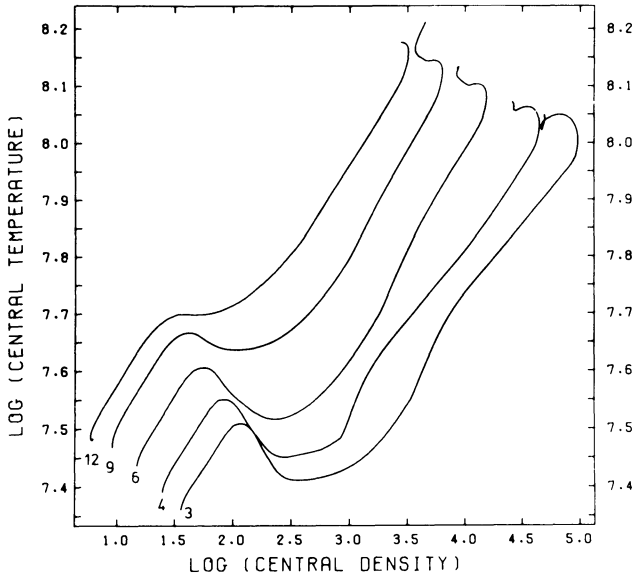


Fig. 3. Central values of density and temperature.

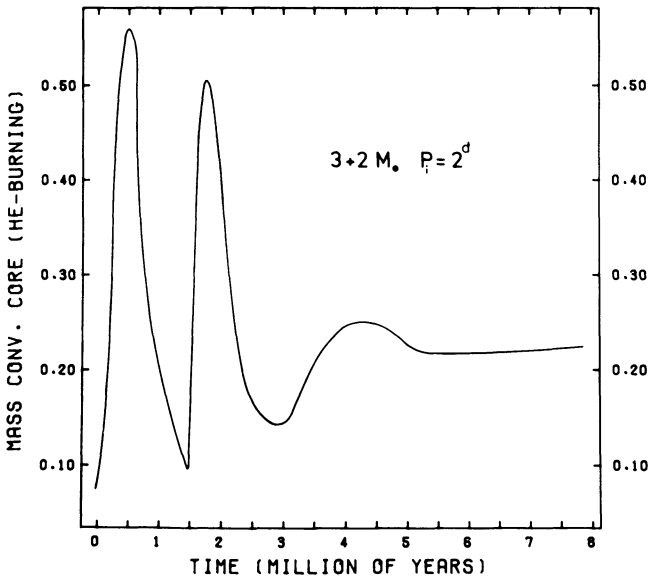


Fig. 4. Relative mass fraction of convective core vs. time, in the remnant of original  $3 M_{\odot}$  primary, after the onset of He-burning.